RSC Advances

ROYAL SOCIETY OF CHEMISTRY

www.rsc.org/advances

Graphical abstract:

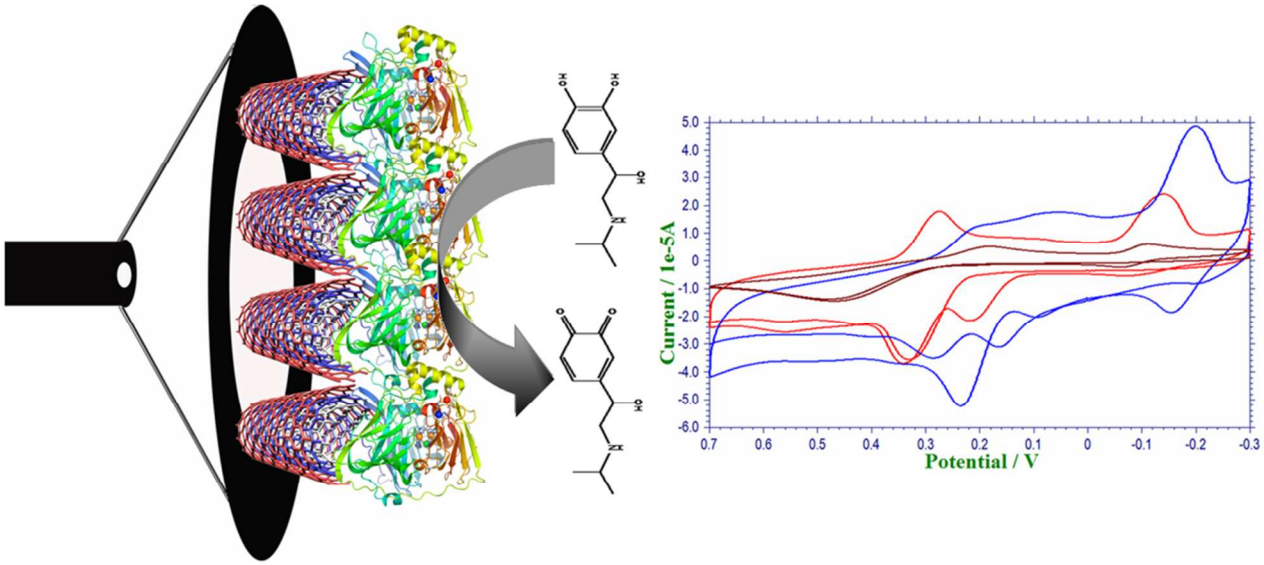

Preparation, characterization and analytical application of electrochemical Laccase biosensor towards the low level determination of Isoprenaline in human serum samples

P. Gopal [a], T. Madhusudana Reddy [a]*, C. Nagaraju [b] and G. Narasimha [c]

[a] *Electrochemical Research Laboratory, Department of Chemistry, S.V.U. College of Sciences, Sri Venkateswara University, Tirupati-517502, Andhra Pradesh, India.*

[b] *Organophosporous research Lab, Department of Chemistry, S.V.U. College of Sciences, Sri Venkateswara University, Tirupati-517502, Andhra Pradesh, India.*

[c] *Applied Microbiology Laboratory, Department of Virology, Sri Venkateswara University, Tirupati 517502, Andhra Pradesh, India*

Abstract

A novel electrochemical biosensor was developed based on the immobilization of multi walled carbon nanotubes (MWCNT) on to the glassy carbon electrode (GCE) and subsequent casting of silca sol-gel (SiSG) entrapment of Laccase (Lac) enzyme on to the MWCNT/GCE. The catalytic activity of laccase biosensor was found to be good enough in sensitive determination of Isoprenaline (ISP) with the aid of voltammetric techniques and we have also demonstrated the detailed electrochemical redox mechanism of ISP. From the effect of the pH, we have optimized the optimum pH as 5.5 and from effect of scan rate; we have evaluated the kinetic parameters, heterogeneous rate constant, charge transfer coefficient and diffusion coefficient values. Furthermore limit of detection (LOD) and limit of quantification (LOQ) values were achieved as 1.8×10^{-7} M and 6.0×10^{-7} M. The simultaneous determination of ISP in the presence of uric acid (UA) and ascorbic acid (AA) was successfully carried out. The surface nature of the biosensor was characterized by using the electrochemical impedance spectroscopy. Finally the validation of the proposed method was verified by the recovery of injection (ISP) in serum sample and their recoveries were found to be in satisfactory range. The proposed method was found to have good repeatability, reproducibility and stability with lower relative standard deviation (RSD) values

Key words: Laccase, Isoprenaline, multi walled carbon nanotubes, biosensor, simultaneous determination and real sample analysis

*Corresponding author E-mail address: *tmsreddysvu@gmail.com, Tel.: +91-877-2289303*

1. Introduction:

Isoprenaline (ISP) (4-[1-hydroxy-2-(isopropylamino)ethyl]benzene-1,2-diol) is also known as Isoproterenol is a catecalamine drug, which has been used for bradycardia or heart block. ISP activates the β1-receptors on the heart and includes positive chronotropic, dromotropic and inotropic effects [1-3]. It was also used for the treatment of primary pulmonary hypertension, status asthmaticus and bronchial asthama [4-7]. ISP can give relaxation from all varieties of smooth muscle when the tone is high [8]. The excessive use of ISP will cause the heart failure and arrhythmias. In 1963, England, Australia, New Zealand and three other countries have encountered a series of deaths, which were associated with repeated and excessive use of ISP inhalation [9, 10]. Therefore on the basis of previous description, there was an essentiality for the development of new sensors for the quantitative determination of ISP levels in human blood samples.

Ascorbic acid (AA) and Uric acid (UA) are the most important electroactive biological compounds present in the human body which plays a potential role in the metabolic system and has similar electrochemical behaviour with catecholamines. Ascorbic acid (AA) is important in health care of human beings. It is especially essential to the skin, connective tissues and immune system. Uric acid (UA) is the final oxidation product of urine metabolism and is excreted in urine [11]. At conventional electrodes the determination of catecholamines in the presence of UA and AA is more of difficult; it results in overlap of voltammetric responses [12, 14]. Due to the adsorption of AA products onto the convention electrodes surface causes surface fouling, poor selectivity and reproducibility [14]. Hence it is a challenging task for the simultaneous determination of ISP, AA and UA. So far a very few mediators have been reported towards the simultaneous determination of ISP, which includes conducting material [15], carbon nanotube paste electrode [7, 16], metal complexes and graphene modified electrodes [3].

Since, from the discovery of CNT's in 1991 by Sumio Iijima, they were emerged as a novel class of nanometerials having applications in chemistry and physics. Due to structural, mechanical, electrical and physical properties of CNT's, they were employed for the preparation

of CNT-modified electrodes. These CNT's will enhances the voltammetric peak height, which facilitates the sensitive determination in analytical sensing, they also reduces the over potential of the system with no surface fouling [18, 19].

Laccases belongs to a group of poly phenol oxidases containing copper atoms in their catalytic center, which are called as multi copper oxidases. These enzymes are widely described in plants, fungi (ascomycetes and basidymocetes) and microorganisms, where they were presumably involved in lignin synthesis and degradation process. Additionally, Laccases can play a role in the fungal virulence by the detection from phytoalexins and tannins. The catalytic center of laccase cluster has four copper atoms and under goes oxidation by oxygen and is brought back to its reduced form by the oxidation of substrate. The four copper atoms of the cluster were classified into type I, type II and type III. Due to its high redox potential (+790 mV) type I copper is the responsible for the catalytic oxidation of molecular oxygen into water and plays a significant role in the oxidation of ortho and para diphenols, polyphenols, aminophenos and polyamines [20, 21]. The schematic representation of enzyme activity is shown in scheme 1.

Scheme 1

There are several reports which have been established for the qualitative and quantitative determination of ISP, such as spectrophotometry [22-25], spectrofluorimetry [26-28], High-performance liquid chromatography (HPLC) [29, 30] and Chemiluminescence [31, 32]. Even though they have better sensitivity and selectivity, they require more expensive experimental procedure, time consuming and solution preparation complications. The electroanalytical methods such as CV and DPV are of simple, rapid and low expensive analytical techniques used in many fields of chemistry, particularly for the development of new sensors towards the monitoring of drugs, pesticides and environmental pollutants [33-35]. In this study we have fabricated an electrochemical Laccase biosensor based on multi walled carbon nanotubes immobilized on glassy carbon electrode.

To the best of our knowledge, there was no work has been reported towards the determination of ISP in the serum samples and its simultaneous determination in the presence of UA and AA, using the fabricated Lac-SiSG/MWCNT/GCE. Therefore in this present study, we have demonstrated electrochemical redox behaviour of ISP at Lac-SiSG/MWCNT/GCE. We have evaluated the quantitative determination of ISP in the phosphate buffer solution (PBS), their

recoveries in the spiked human serum samples and the analytical performance of the developed biosensor towards the simultaneous determination of ISP in the presence of UA and AA.

2. Experimental:

2.1 Materials:

All materials were received from commercial source and used without any further purification. Isoprenaline (ISP) and Tetraethyl orthosilicate (TEOS) were purchased from Sigma-Aldrich and Multiwalled carbon nanotubes (MWCNTs) were from Dropsens, Edificio CEEI, Llanera (SPAIN). Uric acid (UA), Ascorbic acid (AA), $K_4[Fe(CN)_6]$, Triton X-100 and Na_2HPO_4 were from Merck specialties Pvt. Ltd, Mumbai and $K_3[Fe(CN)_6]$, NaH_2PO_4 were from Fisher Scientific India Pvt. Ltd, Mumbai. The Laccase enzyme used in the present study was obtained from applied microbiology laboratory, Department of Virology, S. V. University, Tirupati. This was isolated from fungal culture and from soil contaminated with forest wastes [36].

2.2 Instrumentation:

Cyclic voltammetry (CV), square wave voltammetry (SWV), Chronoamperommetry (CA), Differential pulse voltammetry (DPV) and electrochemical impedance spectroscopy (EIS) techniques were performed by using CH – Electrochemical workstation (Model CHI – 660D, CH Instruments, Austin, USA) with conventional three electrode system made up of saturated calomel electrode (SCE) as a reference electrode, glassy carbon rod as a counter electrode and Lac-SiSG/MWCNT/GCE as a working electrode. The pH solutions were prepared by mixing of 0.1 M NaH_2PO_4 to 0.1 M Na_2HPO_4 using Elico U 120 pH meter combined with pH CL 51 B electrode for measuring the pH values.

2.3 Preparation of MWCNT and Laccase suspention:

1 mg of MWCNT was accurately weighed and dissolved in 2ml of Ethyl alcohol and sonicated by using ultrasonication bath for 10 minutes and stored in refrigerator when not in use. 10 mg of Laccase was accurately weighed and dissolved in 10 mL of Phosphate buffer solution containing pH-6.5 and used as a laccase enzyme stock solution.

2.4 Preparation of silica-solgel/Laccase enzyme:

A homogenous TEOS silica sol–gel was prepared by mixing 4 ml of TEOS, 2 ml of H_2O, 100 µL of 0.1M HCl, 50 µL of 10% Triton- X-100. The mixture was stirred for 1 hr to form a clear sol. The sol can be stored for several days when refrigerated. To the mixture of 20 µL of silica sol-gel and 80 µL of PBS pH-6.5, 50 µL of stock Laccase enzyme solution was added and the solution was stirred well and stored for further use [37].

2.5 Fabrication of Lac-SiSG/MWCNT/GCE:

Prier to modification of glassy carbon electrode (GCE), it was first polished with Al_2O_3 having 1.0, 0.3 and 0.05 micron size to get mirror shine. The polished GCE was used as a bare electrode, and then 5µL of MWCNT suspension was dispersed onto the surface of bare GCE through physical adsorption method and allowed to dry for 5 min to form a MWCNT/GCE.

The obtained MWCNT/GCE was further modified with Laccase enzyme by using sol-gel method. 5 µL of LacSiSG was immobilized on to the MWCNT/GCE and dried for one hour. The obtained electrode was washed with buffer solution and it was denoted as Lac-SiSG/MWCNT/GCE.

\

2.6 Serum sample preparation

The blood sample was collected from good healthy person having age around 35 years, and was kept aside for ½ hour and centrifuged for about 10 minutes with 3000 rpm. The supernatant serum was collected and stored for further use. To the 0.3 mL of serum sample, 3 mL of ethyl alcohol was added and centrifuged for 5 minutes with 3000 rpm, the obtained protein free serum was collected and was used for further analysis.

3. Results and Discussion:

3.1 Voltammetric characterization of electrodes with $K_3[Fe(CN)_6]$:

The voltammetric responses of bare GCE, MWCNT/GCE and Lac-SiSG/MWCNT/GCE was examined in 1.0×10^{-3} M $[Fe(CN)_6]^{-3}$ in 1 M KCl solution by using CV technique. Fig. 1 is the CV response for $[Fe(CN)_6]^{-3}$ at bare GCE, MWCNT/GCE and Lac-SiSG/MWCNT/GCE with a scan rate of 0.1 V. At bare electrode, the peak currents of $[Fe(CN)_6]^{-3}$ was $i_p^a = -1.452 \times 10^{-5}$ A with $\Delta E_p = 80$ mV. At MWCNT/GCE, the peak currents of $[Fe(CN)_6]^{-3}$ enhanced to $i_p^a = -1.81 \times$

10^{-5} A with decrease in peak separation of ΔE_p= 70 mV, this was the clear indication for the catalytic activity of MWCNT modified GCE. Due to the presence of large surface area and high electrical conductivity properties of MWCNTs, an increase in the peak currents was observed at MWCNT/GCE. Furthermore at Lac-SiSG/MWCNT/GCE, the peak currents of $[Fe(CN)_6]^{-3}$ was increased to $i_p^a = -2.117 \times 10^{-5}$ A in comparison with bare GCE and MWCNT/GCE and this was due to the presence of enhanced catalytic surface area than MWCNT/GCE, that leading to the fast electron transfer. The anodic peak current i_p^a and cathodic peak current i_p^c ratio for $[Fe(CN)_6]^{-3}$ at three different electrodes were nearly unity, indicates the good reversibility of $[Fe(CN)_6]^{-3}$. The effect of scan rate was observed and the peak currents were directly proportional to the $\upsilon^{1/2}$, indicating that the process was under diffusion control. Based on the scan rate results and by employing the equations (1) and (2), we have evaluated diffusion coefficient (D) and active surface coverage area (Γ) of different electrodes and the values were listed in table.1 [38, 39]. Where 'n' is the number of electrons, 'C' is the concentration (mol cm^{-3}), 'υ' is the scan rate (V s^{-1}), and 'F' is the Faraday constant (96485 c mol^{-1}).

$$i_p = 2.69 \times 10^5 n^{3/2} D^{1/2} C \upsilon^{1/2} \quad (1)$$

$$i_p = n^2 F^2 \upsilon A \Gamma / 4RT \quad (2)$$

Fig.1 and Table.1

3.2 EIS characterization of electrodes with Ferri/Ferro:

EIS technique was the most power full non-destructive and investigative tool for the characterization of surface nature of different electrodes. The EIS spectrum exhibits semicircular and linear portions, the semicircular part represents the charge transfer resistance (R_{ct}) and linear part describes the low electron transfer rate. In this study we have studied the surface nature of bare GCE, MWCNT/GCE and Lac-SiSG/MWCNT/GCE electrodes at ferri and ferro probe in 1M KCl solution. Fig. 2a was the Nyquist plots for bare GCE, MWCNT/GCE and Lac-SiSG/MWCNT/GCE, from the figure the bare electrode was having more charge transfer resistance (R_{ct}) than the other two electrodes and the Lac-SiSG/MWCNT/GCE was having least charge transfer resistance than the other two, indicating good electron transfer rate at the Lac-SiSG/MWCNT/GCE. Fig. 2b was the bode plot for the corresponding bare GCE, MWCNT/GCE and Lac-SiSG/MWCNT/GCE. The equivalent circuit data was listed in table. 2 [40].

Fig. 2a, Fig. 2b and Table. 2

3.3 Electrochemistry of Isoprenaline at Lac-SiSG/MWCNT/GCE:

To study the electrochemical redox mechanism of ISP, we have recorded CV's of 1 mM ISP in PBS solution of pH-6.5. The scan was performed for three segments between the potential ranges from -0.3 V to 0.7 V. The CV's of ISP depicts that, in the first segment i.e. from -0.3 V to 0.7 V ISP was found to produce only one oxidation peak at potential ≈ 0.237 V and this was due to the oxidation of dihydroxy group present in the ISP to the corresponding dione derivative. In reverse scan i.e. from 0.7 V to -0.3 V, a reduction peak was observed at potential ≈ 0.202 V which was due to the reversible reduction of dione derivative into ISP. The formed dione derivative at potential ≈ 0.237 V was found to undergo 1, 4-Michels addition reaction to form a cyclization product that in turn goes for reduction process at the potential -0.2 V to form the corresponding dihydroxy cyclization product. In the third segment i.e. from -0.3 to 0.7 V there was an oxidation peak at the potential -0.16 V which was due to the reversible oxidation of dihydroxy cyclization product to cyclization product. At the potential 0.162 V a small oxidation peak was observed and this was due to the reductive elimination of water molecule. The electrochemical redox reaction mechanism was shown in scheme. 2 [41-43]. Fig. 3 was the CV responses of ISP at bare GCE, MWCNT/GCE, Lac-SiSG/MWCNT/GCE. From the CV responses, it was observed that there was an increase in the peak currents at MWCNT/GCE in comparison with bare GCE, which was due to the catalytic nature of the MWCNTs immobilized on the surface of the GCE. Further the peak current of ISP at Lac-SiSG/MWCNT/GCE was enhanced in comparison with bare GCE and MWCNT/GCE and this was due to the catalytic nature of copper atoms present in the Laccase enzyme.

Fig. 3 and Scheme. 2

3.4 Effect of pH:

The effect of pH values of the supporting electrolyte (PBS) ranging from pH-4.5 to 8.0 was studied on the response of peak currents and peak potentials of ISP at Lac-SiSG/MWCNT/GCE with SWV technique. The pH of the supporting electrolyte was greatly influencing the peak currents and peak potential response of ISP. It was noticed that when the pH of the electrolyte was increased from lower value, the peak currents of ISP was found to increase up to the pH value of 6.5, above this value the peak currents stared to decline and it may be due to the unavailability of protons in basic medium which leads to unfavorable condition for the

electrochemical redox reaction of ISP. At pH 6.5 we noticed high peak currents of ISP with less peak potentials; hence we have selected the pH 6.5 as optimum pH. The peak potentials was found to shift to the nearer value of zero with increase in the pH of the supporting electrolyte, indicating the involvement of protons in the electrochemical reaction. Fig. 4 shows that the graphical representation of peak currents verses pH and peak potentials verses pH, the linear regression equation for the peak potentials against the function of pH was found to be as E_p (V)= 0.527 - 0.061 pH. The slope of the linear regression equation was nearly 0.059 V indicating the involvement of equal number of protons and electrons [44].

Fig. 4

3.5 Effect of scan rate:

In order to determine the kinetic parameters of ISP at Lac-SiSG/MWCNT/GCE, we have studied the effect of scan rates between the ranges from 0.01 V to 0.15 V with CV by taking 1mM ISP in PBS solution of pH 6.5. It was observed that the peak currents of ISP was linearly increasing against $\upsilon^{1/2}$, indicating diffusion controlled process with linear regression equation of $I_p^c{}_1$ (μA) = 0.662 (μA) + 17.394 $\upsilon^{1/2}$ (υ in V) with correlation factor r = 0.998. Fig. 5a was the CV's of ISP with different scan rates from 0.01 V to 0.15 V and Fig. 5b is a linear plot of peak currents against square root of scan rate [45, 46]. Based on the equations (3) and (4) we have determined the charge transfer coefficient 'α' as 0. 39 and heterogeneous rate constant 'k_s' as 1.41 × 10^{-3} cm^{-1}. Where 'n' is the number of electrons involved in the rate determining step and 'α' is the charge transfer coefficient, 'D' is the diffusion coefficient and 'm' is the slope of the Ep Vs ln υ.

$$E_p = E^0 - m\,[0.78 + \ln(D^{1/2}/k_s) + (m/2)(\ln m)] + m/2 \ln \upsilon \qquad (3)$$

$$m = RT/(1-\alpha)nF \qquad (4)$$

Fig. 5a and Fig. 5b

3.6 Effect of concentration:

CA is the more sensitive technique, which gives information about the peak currents at low concentration levels. In this study we have studied the concentration effect on the peak currents of ISP in PBS at Lac-SiSG/MWCNT/GCE. The slope values of CA curves were linearly increasing with increase in the concentration of the ISP. Fig. 6a represents the chronoamperomtric

responses of different ISP concentrations and insert is the short view for CA's. Fig. 6b shows the linear dependence of slope values from CA against the concentration of ISP ranging from 5×10^{-6} M to 6×10^{-4} M and the linear regression equations were found to be as follows

$$\text{Slope} = 5.65 + 0.064\ C\ (\mu M)$$

$$\text{Slope} = 6.16 + 0.086\ C\ (\mu M)$$

The limit of detection (LOD) and limit of quantification (LOQ) values were evaluated from the slopes of above equations and using following equations 5 & 6, where 'S' is the standard deviation and 'm' is the slope for the calibration curve, the LOD and LOQ values were 1.8×10^{-7} M and 6.0×10^{-7} M [47] respectively. The LOD and linear detection range (LDR) values of ISP with other methods were compared in table. 3.

$$LOD = 3S/m \quad \text{-------} \quad (5)$$

$$LOQ = 10S/m \quad \text{-------} \quad (6)$$

Fig. 6a, Fig. 6b and Table. 3

3.7 Simultaneous determination of ISP in the presence of UA and AA:

The simultaneous determination of ISP in the presence of biologically important molecules such as UA and AA is of challenging task, because the oxidation potentials of ISP, UA and AA are very closer to each other. The selectivity and resolution of ISP, UA and AA at the Lac-SiSG/MWCNT/GCE is of great interest. Therefore the main objective of the present study was to determine ISP in the presence of UA and AA in PBS buffer and as well as PBS buffer spiked with serum samples. The fabricated electrode can resolve well all the three compounds separately with good sensitivity in comparison with MWCNT/GCE.

Fig. 7a shows the increase in the peak currents of ISP in PBS buffer at potential ≈ 0.2 V with a constant increase in the ISP concentration from 5 μM to 45 μM, in the presence of UA (4 μM) and AA (200 μM), from the figure we could see that there was no influence of ISP concentration on the UA and AA. Fig. 7b shows the constant increase of peak currents of UA with the increment in the concentration from 5 μM to 50 μM in the presence of constant volumes of ISP (12 μM) and AA (200 μM), from this result we could notice that there was no influence of UA concentration on the ISP and AA. Fig. 7c shows the increase in the peak currents of AA with the constant increase in the concentration from 50 μM to 350 μM in the presence of constant concentration of ISP (4 μM) and UA (4 μM), from this figure we could notice that there was a

slight positive shift in the peak potentials of ISP and UA, this may be due to the more acidic nature of AA. As the concentration of AA was increased, the pH of the solution changes to less pH values and causes the shift. We have studied the non-interfering concentration range of UA and AA against ISP, were we could notice that there was no interference of UA concentration from 20 – 1000 μM against 10 μM of ISP and also on further increase of UA concentration beyond 1000 μM there was no influence on the electrochemical signal tendency of ISP, on the other hand as the concentration of AA was increased there was an influence on ISP signal.

Fig. 7d shows the increase in the peak currents at potential ≈ 0.1 V for ISP in PBS buffer spiked with human serum sample. ISP concentration was increased gradually from 1 μM to 100 μM, in the presence of UA (10 μM) and AA (150 μM), a linear relation was observed between the peak currents and different concentrations of ISP, the linear equation was found to be as i_p (μA) = 0.3056 (μA) + 0.0111 C_{ISP} (μM). Based on the linear equation the limit of detection value was determined as 2.3 μM. Fig. 7e shows the increase of peak currents of UA with the increment in the concentrations of UA ranging from 6 μM to 80 μM under the constant volumes of ISP (20 μM) and AA (150 μM) and insert of the figure was the plot drawn between the peak currents and different concentrations of UA, a linear equation was observed as i_p (μA) = 0.1108 (μA) + 0.0168 C_{UA} (μM) and the detection limit for UA in the presence of ISP and AA was 4.7 μM. Fig. 7f shows the increment in the peak currents of AA with the constant increase in the concentration from 20 μM to 240 μM with constant concentration of ISP (5 μM) and UA (10 μM) and the insert of the figure was the plot drawn between the peak currents and concentrations of AA, a linear equation i_p (μA) = -0.1163 (μA) + 0.0076 C_{AA} (μM) was observed and from the linear equation the limit of detection value was achieved as 27.4 μM. From the Fig. 7c, we could clearly see that there was an influence of AA on the ISP and UA in the pure PBS buffer, but whereas from Fig 7f, we could see that there was no much influence of AA on the ISP and UA in PBS buffer spiked with human serum samples, this may be due to the change in the pH of the supporting electrolyte.

Fig. 7a, Fig. 7b, Fig. 7c, Fig. 7d, Fig. 7e and Fig. 7f

3.8 Recoveries from pharmaceutical formulation and serum samples:

The developed method was effectively used for the determination of ISP in injection samples and the concentration of ISP in the injection samples was verified by using standard addition method. Firstly, the collected ISP injection sample was diluted to required concentration

and same concentration was prepared with the standard drug sample. The recoveries for different concentrations of injection samples were in the rage from 101 % to 104 % and the values were listed in table.4. The recoveries of ISP injection in serum sample were studied by using the standard addition method and were listed in table. 4. The recovery values suggested that the proposed biosensor was in satisfactory condition.

Table. 4

3.9 Repeatability, Reproducibility and stability:

To find the practical utilization of the fabricated biosensor, we have studied repeatability, reproducibility and stability. The developed biosensor was tested with 1mL of 10 mM ISP in 9 mL of pH-6.5 PBS using CV and the responses were recorded for several times. The CV responses of each repeated cycle for ISP was nearly the same and had a low RSD value, i.e., 4.22 % indicating good reproducibility of the fabricated biosensor. Fig. 8 was the CV's of 1 mM ISP in PBS pH-6.5 with the scan rate of 100 mVs^{-1} and the insert was the plot between the peak currents and number of measurements.

The biosensor electrode was prepared for four times and recorded the CV responses for 1 mL of 10 mM ISP in 9 mL of pH-6.5 PBS. The current responses of four different electrodes were almost same with less relative standard deviation (RSD). The proposed biosensor was continuously tested for 50 successive cycles with a scan rate of 100 mV/s containing 1mL of 10 mM ISP in 9 mL of PBS pH-6.5. The relative standard deviation of the CV responses was suggesting that the developed biosensor was found to have good stability [46].

Fig. 8

4. Conclusions:

Here in, we have demonstrated the electrochemical redox behaviour of ISP at Lac-SiSG/MWCNT/GCE biosensor. The fabricated biosensor was found to exhibit a good electrochemical catalytic ability to determine ISP with lower detection limits. The fabricated biosensor had the capability for the determination of ISP in the presence of UA and AA simultaneously. Moreover the practical applicability of the developed electrode was examined in human serum samples with satisfactory results. Finally this study will facilitate a simple and

versatile protocol for the monitoring of ISP concentrations with good repeatability, reproducibility and stability.

Acknowledgments:

One of the authors P. Gopal gratefully acknowledges the University grant commission (UGC) for providing financial support through Basic scientific research (BSR)-Research fellowship for meritorious students.

References:

1. H. Beitollahi, I. Sheikhshoaie, Electrochim. Acta, 2011, **56,** 10259– 10263.
2. V. G. Bonifacio, L. H. Marcolino Jr, M. F.S. Teixeira, O. F. Filho, Microchem. J., 2004, **78,** 55– 59.
3. M. Chen, X. Ma, X. Li, J. Solid State Electrochem., 2012, **16**, 3261–3266.
4. A. Kutluay, M. Aslanoglu, Acta Chim. Slov. 2010, **57**, 157–162.
5. C. Bian, Q. Zeng, H. Xiong, X. Zhang, S. Wang, Bioelectrochemistry, 2010, **79,** 1–5.
6. Y. Ni, M. Wei, S. Kokot, Int. J. Bio. Macromol., 2011, **49**, 622– 628.
7. A. A. Ensafi, H. K. Maleh, Int. J. Electrochem. Sci, 2010 **5**, 1484 – 1495.
8. L.S. Goodman, A. Gilman, The Pharmacological Basis of Therapeutics, ninth ed., McGraw-Hill, New York, 1996, pp. 105–120.
9. N. Pearce, M. J. Hensley, Epidemiol. Rev., 1998, **20**, 173 – 186.
10. Code of Federal Regulations, Title 21, Food and Drugs: Parts 200-299.
11. D. Han, T. Han, C. Shan, A. Ivaska, L. Niua, Electroanalysis 2010, **22**, 2001 – 2008.
12. J. Ping, J. Wu, Y. Wang, Y. Ying, Biosens. Bioelectron., 2012 **34**, 70–76.
13. M. M. Ardakani, L. Hosseinzadeh, A. Khoshroo, H. Naeimi, M. Moradian, Electroanalysis 2014, **26**, 275 – 284.
14. H. Beitollahia, I. Sheikhshoaieb, Electrochim. Acta, 2011 **56**, 10259–10263.
15. A. A. Ensafi, M. Dadkhah, H. K. Maleh, Colloids Surf., B, 2011, **84**, 148–154.
16. A. A. Ensafi, H. Bhrami, H. K. Maleh, S. Mallakpour, Chin. J. Catal., 2012, **33**, 1919–1926.
17. X. Yang, B. Feng, X. He, F. Li, Y. Ding, J. Fei, Microchim. Acta, 2013, **180**, 935–956.
18. M. Keyvanfard, V. Khosravi, H. K. Maleh, K. Alizad, B. Rezaei, J. Mol. Liq., 2013, **177**, 182–189.
19. B. J. Sanghavi, A. K. Srivastava, Electrochim. Acta, 2011, **56,** 4188–4196.
20. D. Monti, G. Ottolina, G. Carrea, S. Riva, Chem. Rev., 2011, **111**, 4111–4140.
21. C. Tortolini, S. Rea, E. Carota, S. Cannistraro, F. Mazzei, Microchem. J., 2012, **100**, 8–13.
22. H. Jeon, H. Nohta, H. Nagaoka, Y. Ohkura, Anal. Sci., 1991, **7**, 257.
23. H. Nohta, T. Yukizawa, Y. Ohkura, M. Yoshimura, J. Ishida, M. Yamaguchi, Anal. Chim. Acta, 1997, **344**, 233.

24. G. Alberts, T. Lameris, A. H. V. Meiracker, A. J. M. I. Veld, F. Boomsma, J. Chromatogr. B, 1999, **730**, 213.
25. R. M. V. Camanas, J. M. S. Mallols, J. R. T. Lapasio, V. R. Ramos, Analyst, 1995, **120,** 1767.
26. K. O. Lupetti, I. C. Vieira, O. F. Filho, Talanta, 2002, **57,** 135.
27. P. Solich, C. K. Polydorou, M. A. Koupparis, C. E. Efstathiou, J. Pharm. Biomed. Anal., 2000, **22**, 781.
28. J. J. B. Nevado, J. M. L. Gallego, P. B. Laguna, Anal. Chim. Acta, 1995, **300**, 293.
29. Y. Qu, L. F. Moons, F. Vandesande, J. Chromatogr. B. Appl., 1997, **704,** 351.
30. F. Mashige, Y. Matsushima, C. Miyata, R. Yamada, H. Kanazawa, I. Sakuma, N. Takai, N. Shinozuka, A. Ohkubo, K. Nakahara, Biomed. Chromatogr., 1995, **9,** 221.
31. G.J. Zhou, G.F. Zhang, H.Y. Chem, Anal. Chim. Acta, 2002, **463,** 257.
32. C. Zhang, J. Huang, Z. Zhang, M. Aizawa, Anal. Chim. Acta, 1998, **374,** 105.
33. P. V. Narayana, T. M. Reddy, P. Gopal, K. Reddaiah, P. Raghu, Res. J. Chem. Sci., 2014, **4**, 37-43.
34. P. Raghu, T. M. Reddy, K. Reddaiah, B.E. K. Swamy, M. Sreedhar, Food Chem., 2014, **142,** 188–196.
35. P. Raghu, M. R. M. Reddy, T. M. Reddy, B. E. K. Swamy, K. Reddaiah, Anal. Bioanal. Electrochem., 2012, **4**, 1 – 16.
36. B. Viswanath, B. Rajesh, A. Janardhan, A. Praveen Kumar, G. Narasimha, Enzyme Research, doi. 10.1155/2014/163242
37. P. Raghu, B.E. K. Swamy, T. M. Reddy, B.N. Chandrashekar, K. Reddaiah, Bioelectrochemistry, 2012, **83**, 19–24.
38. K. Reddaiah, T M. Reddy, P. Raghu, P. Gopal, Anal. Bioanal. Electrochem., 2012, **4** 372-385.
39. P. Raghu, T. M. Reddy, K. Reddaiah, L.R. Jaidev, G. Narasimha, Enzyme and Microb. Technol., 2013, **52,** 377– 385.
40. K. Reddaiah, M. M. Reddy, P. Raghu, T. M. Reddy, Colloids Surf., B, 2013, **106**, 145–150.
41. R. N. Goyal, A. R. S. Rana, H. Chasta, Electrochim. Acta, 2012, **59**, 492– 498.

42. Z. Wang, Z. Zhang, Z. Fu, L. Fang, W. Luo, D. Chen, X. Zhang, Anal. Chim. Acta, 2003, **494,** 63–70.
43. K. Reddaiah, T. M. Reddy, P. Raghu, J. Electroanal. Chem., 2012, **682,** 164–171.
44. K. Reddaiah, T. M. Reddy, Y. S. Rao, P. Raghu, P. Gopal, Mater. Sci. Eng., B, 2014, **183**, 69–77.
45. P. Gopal, T. M. Reddy, K. Reddaiah, P. Raghu, P.V. Narayana, J. Mol. Liq., 2013, **178,** 168–174.
46. P. Raghu, T. M. Reddy, P. Gopal, K. Reddaiah, N.Y. Sreedhar, Enzyme and Microb. Technol., 2014, **57,** 8– 15.
47. J. Uhrovcik, Talanta, 2014, **119**, 178–180.
48. M. Yamaguchi, J. Ishida, M. Yoshimura, Analyst, 1998, **123** 307.
49. A.A. Ensafi, H. Karimi-Maleh, Drug Test. Anal., 2011, **3** 325–330.

Figure captions:

Fig. 1 is the CV responses of 1 mM $[Fe(CN)_6]^{-3}$ in 0.1 M KCl solution with a scan rate of 100 mV s^{-1} at bare GCE ('a' without $[Fe(CN)_6]^{-3}$ and 'b' with $[Fe(CN)_6]^{-3}$), MWCNT/GCE (c) and Lac-SiSG/MWCNT/GCE (d).

Fig. 2a is the Nyquist plot for bare GCE (a), MWCNT/GCE (b) and Lac-SiSG/MWCNT/GCE (c) in $[Fe(CN)_6]^{-3}/[Fe(CN)_6]^{-4}$ probe containing in 0.1 M KCl.

Fig. 2b is the bode plot for bare GCE (a), MWCNT/GCE (b) and Lac-SiSG/MWCNT/GCE (c) in $[Fe(CN)_6]^{-3}/[Fe(CN)_6]^{-4}$ dissolved in 0.1 M KCl.

Fig. 3 is the CV's of 1 mM ISP in PBS of pH-6.5 at bare GCE (a), MWCNT/GCE (b) and Lac-SiSG/MWCNT/GCE (c) with a scan rate of 100 mV s^{-1}

Fig. 4 is the plot drawn between the peak currents, peak potentials (V) and its pH values.

Fig. 5a is the CV's of 1 mM ISP in PBS solution of pH-6.5 at Lac-SiSG/MWCNT/GCE with scan rates of 10 mV s^{-1} (a), 20 mV s^{-1} (b), 30 mV s^{-1} (c), 40 mV s^{-1} (d), 50 mV s^{-1} (e), 60 mV s^{-1} (f), 70 mV s^{-1} (g),80 mV s^{-1} (h), 90 mV s^{-1} (i), 100 mV s^{-1} (j), 110 mV s^{-1} (k), 120 mV s^{-1} (l), 130 mV s^{-1} (m), 140 mV s^{-1} (n) and 150 mV s^{-1} (o)

Fig. 5b is plot between the peak currents (μA) verses their corresponding square root of scan rates $((V/s)^{-1/2})$

Fig. 6a is chronoamperometric responses of ISP with different concentrations 4 μM (a), 7 μM (b), 11 μM (c), 15 μM (d), 25 μM (e), 35 μM (f), 50 μM (g), 70 μM (h), 100 μM (i), 140 μM (j), 200 μM (k), 250 μM (l), 300 μM (m), 350 μM (n), 400 μM (o), 500 μM (p) and 600 μM (q) at Lac-SiSG/MWCNT/GCE.

Fig. 6b is the plot between the slope values of chronoamperometric curves and their peak currents.

Fig. 7a is the DPV's representing simultaneous determination of ISP with different concentrations 5 μM (a), 10 μM (b), 15 μM (c), 20 μM (d), 25 μM (e), 30 μM (f), 35 μM (g), 40 μM (h), 45 μM in the presence of UA (4 μM) and AA (200 μM) at Lac-SiSG/MWCNT/GCE.

Fig. 7b is the DPV's representing simultaneous determination of UA with different concentrations 5 μM (a), 10 μM (b), 15 μM (c), 20 μM (d), 25 μM (e), 30 μM (f), 35 μM (g), 40 μM (h), 45 μM (i) and 50 μM (j) in the presence of ISP (12 μM) and AA (200 μM) at Lac-SiSG/MWCNT/GCE.

Fig. 7c is the DPV's representing simultaneous determination of AA with different concentrations 50 μM (a), 100 μM (b), 150 μM (c), 200 μM (d), 250 μM (e), 300 μM (f), 350 μM (g) in the presence of UA (4 μM) and ISP (4 μM) at Lac-SiSG/MWCNT/GCE.

Fig. 7d is the DPV's for ISP in PBS buffer spiked with human serum samples with different concentrations 1 μM (a), 3 μM (b), 5 μM (c), 7 μM (d), 9 μM (e), 11 μM (f), 15 μM (g), 20 μM (h), 25 μM (i), 30 μM (j), 40 μM (k), 50 μM (l), 60 μM (m), 80 μM (n) and 100 μM (o), in the presence of UA (10 μM) and AA (150 μM) at Lac-SiSG/MWCNT/GCE.

Fig. 7e is the DPV's for UA in PBS buffer spiked with human serum samples with different concentrations 6 μM (a), 8 μM (b), 10 μM (c), 12 μM (d), 14 μM (e), 16 μM (f), 20 μM (g), 25 μM (h), 30 μM (i), 40 μM (j), 50 μM (k), 60 μM (l), 70 μM (m), 80 μM (n) in the presence of ISP (20 μM) and AA (150 μM) at Lac-SiSG/MWCNT/GCE.

Fig. 7f is the DPV's for AA in PBS buffer spiked with human serum samples with different concentrations 20 μM (a), 40 μM (b), 60 μM (c), 80 μM (d), 100 μM (e), 120 μM (f), 140 μM (g), 180 μM (h) and 240 μM (i) in the presence of UA (4 μM) and ISP (4 μM) at Lac-SiSG/MWCNT/GCE.

Fig. 8 is the CV's of 30 replications corresponding to 1 mM ISP in PBS solution of pH-6.5 with a scan rate of 100 mV s^{-1}. Insert is the graphical representation of number of measurements against their peak currents.

Figures:

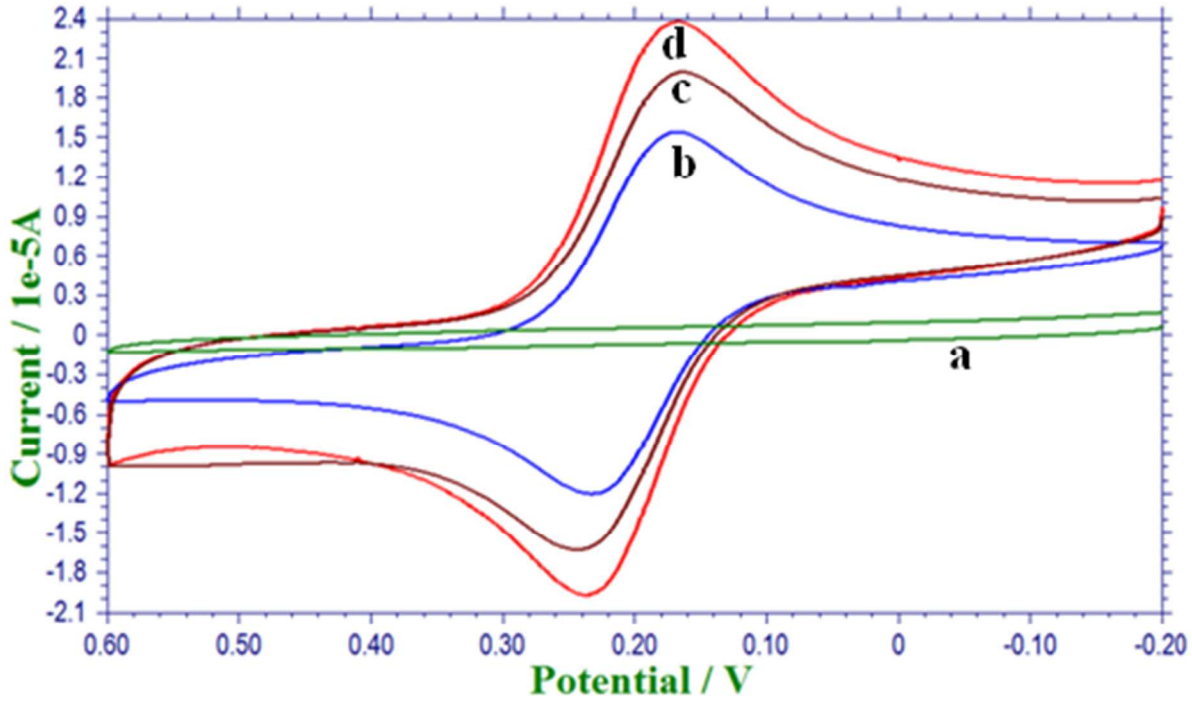

Fig. 1

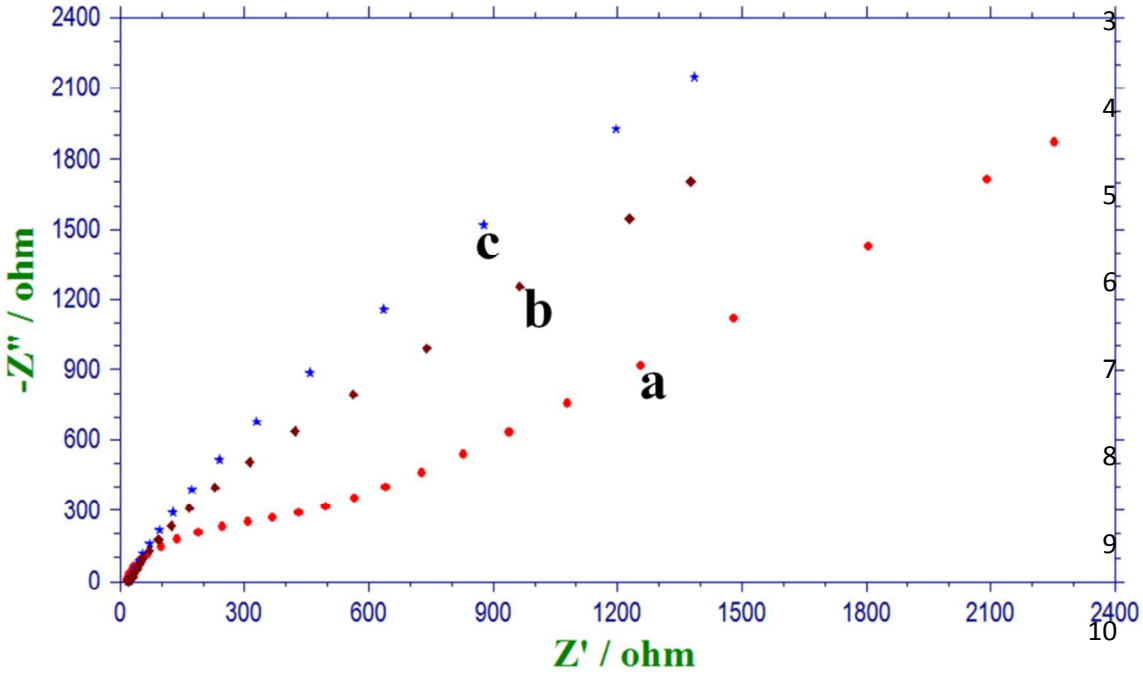

Fig. 2a

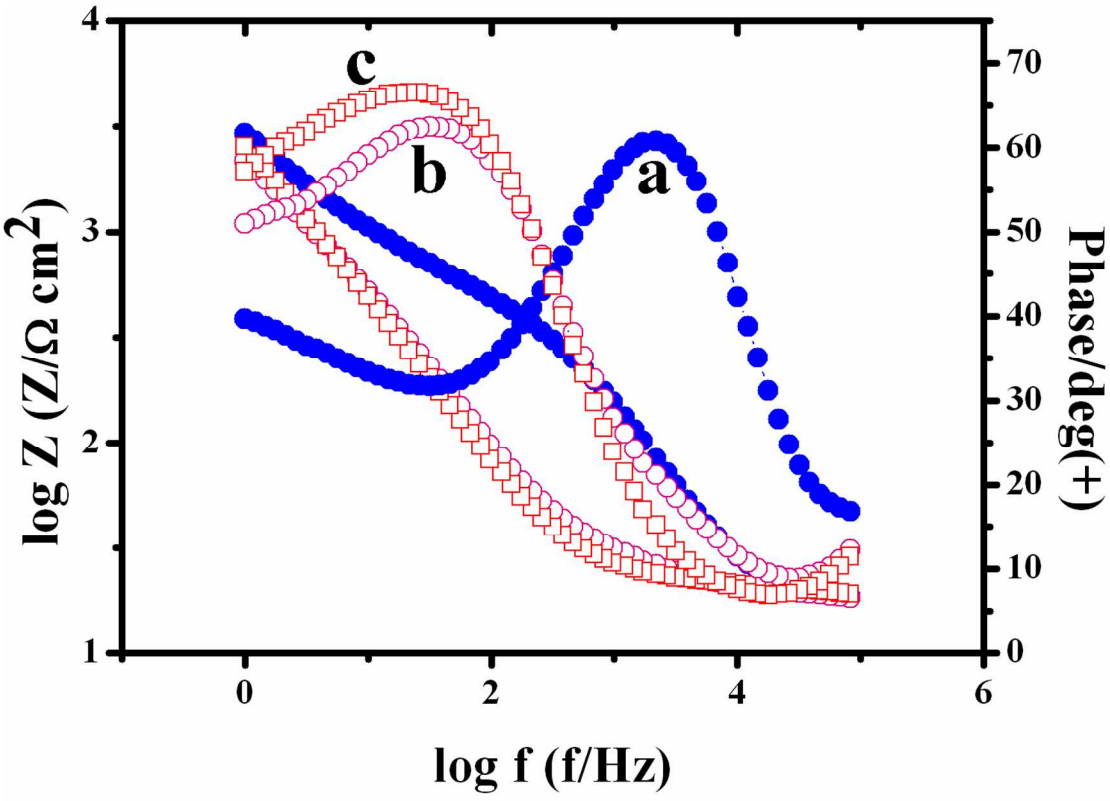

Fig. 2b

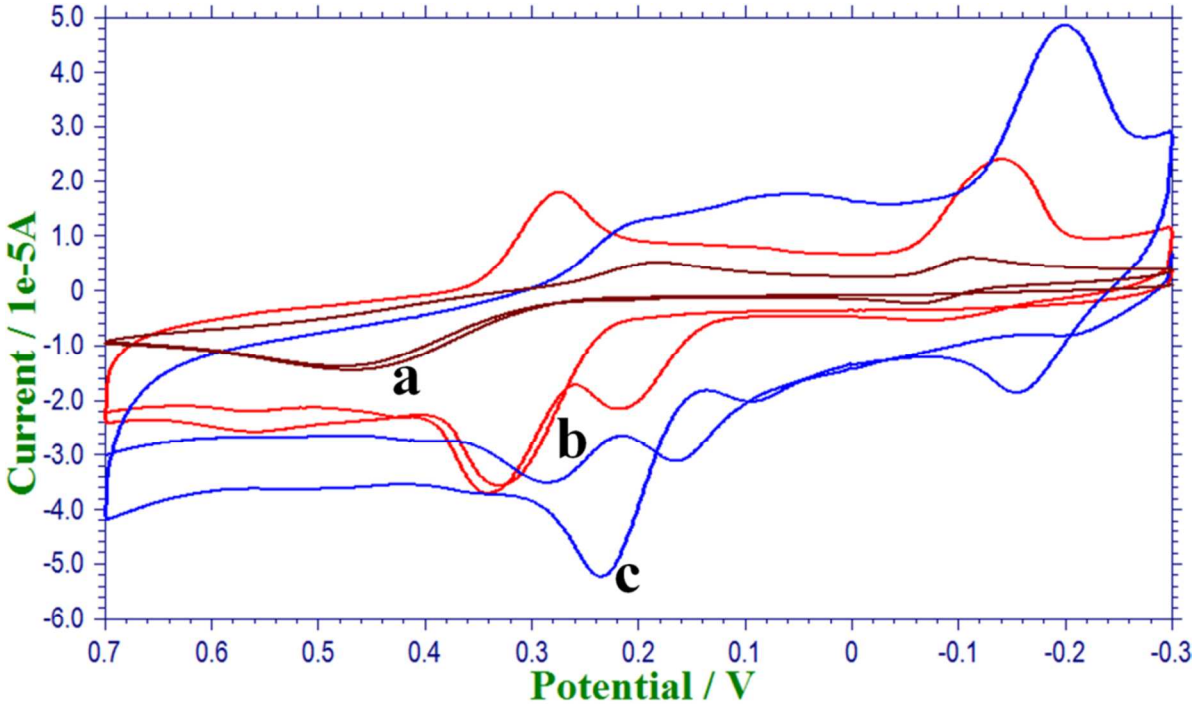

Fig. 3

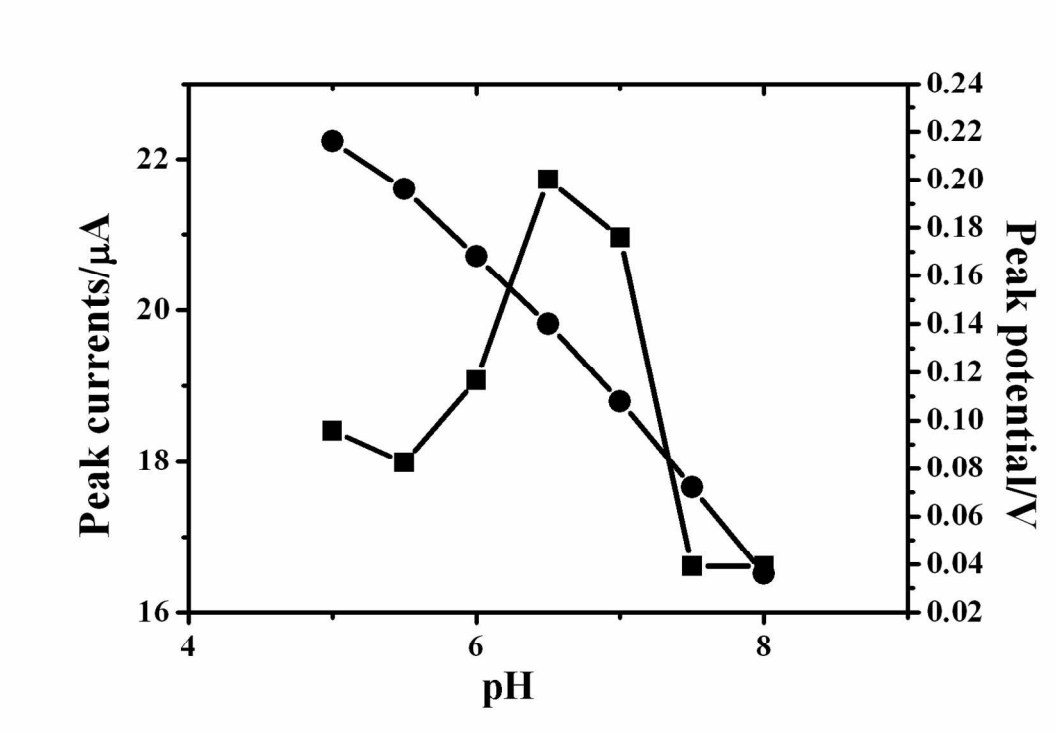

Fig. 4

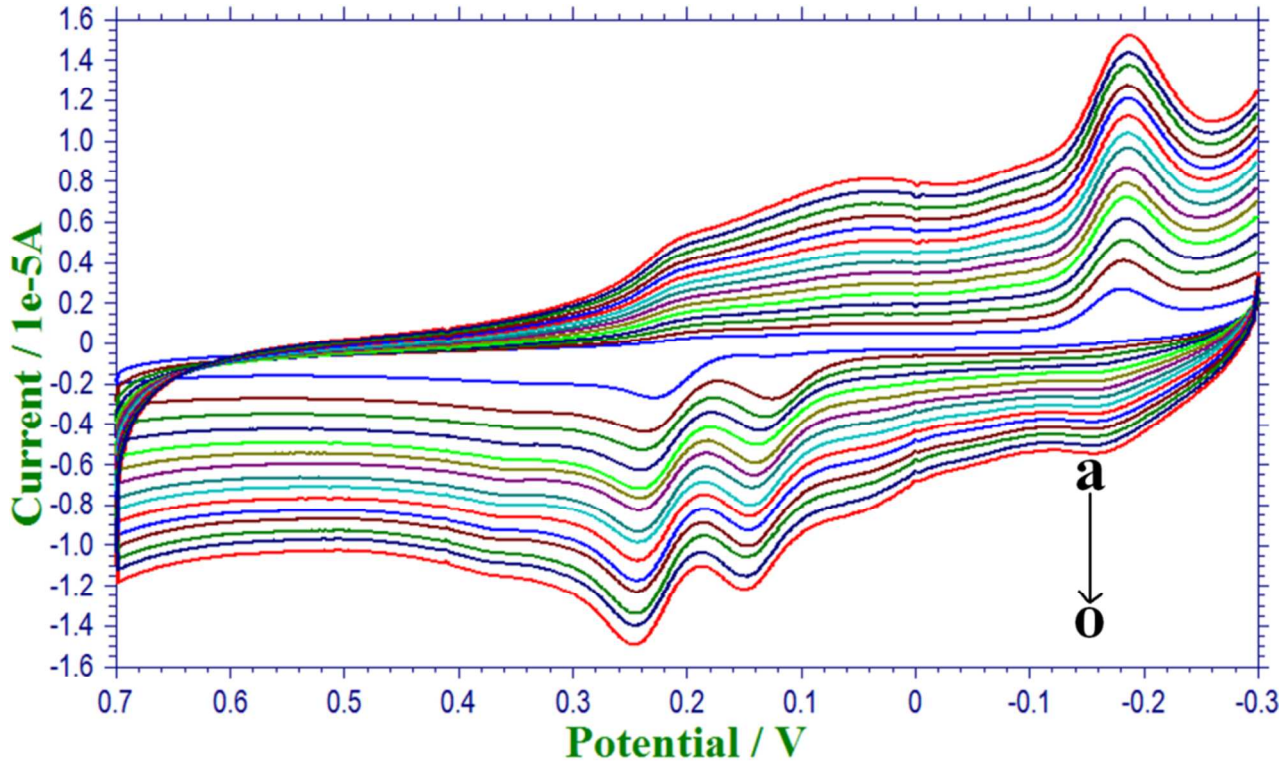

Fig. 5a

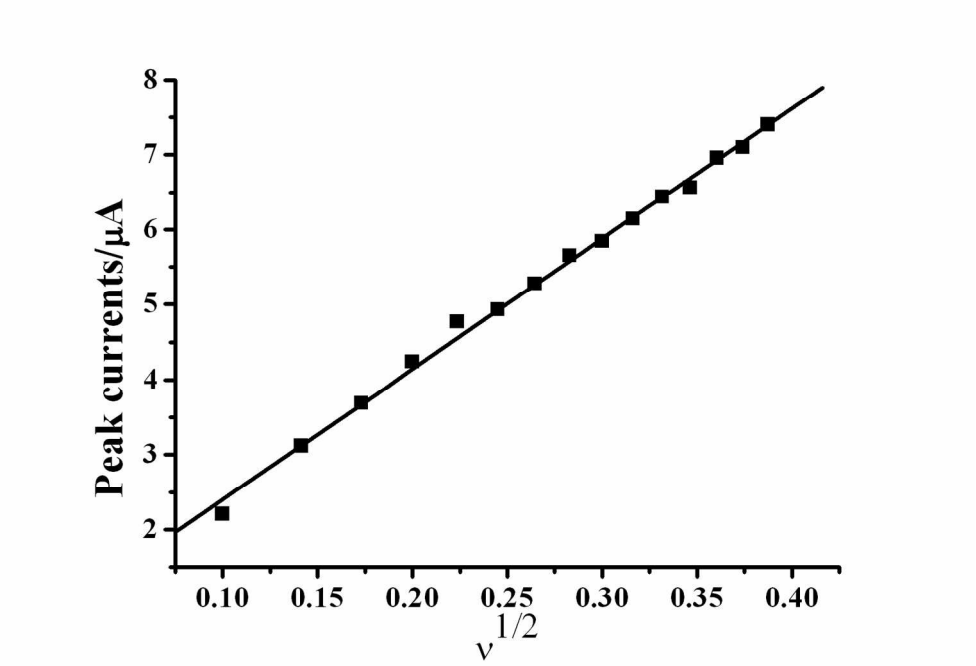

Fig. 5b

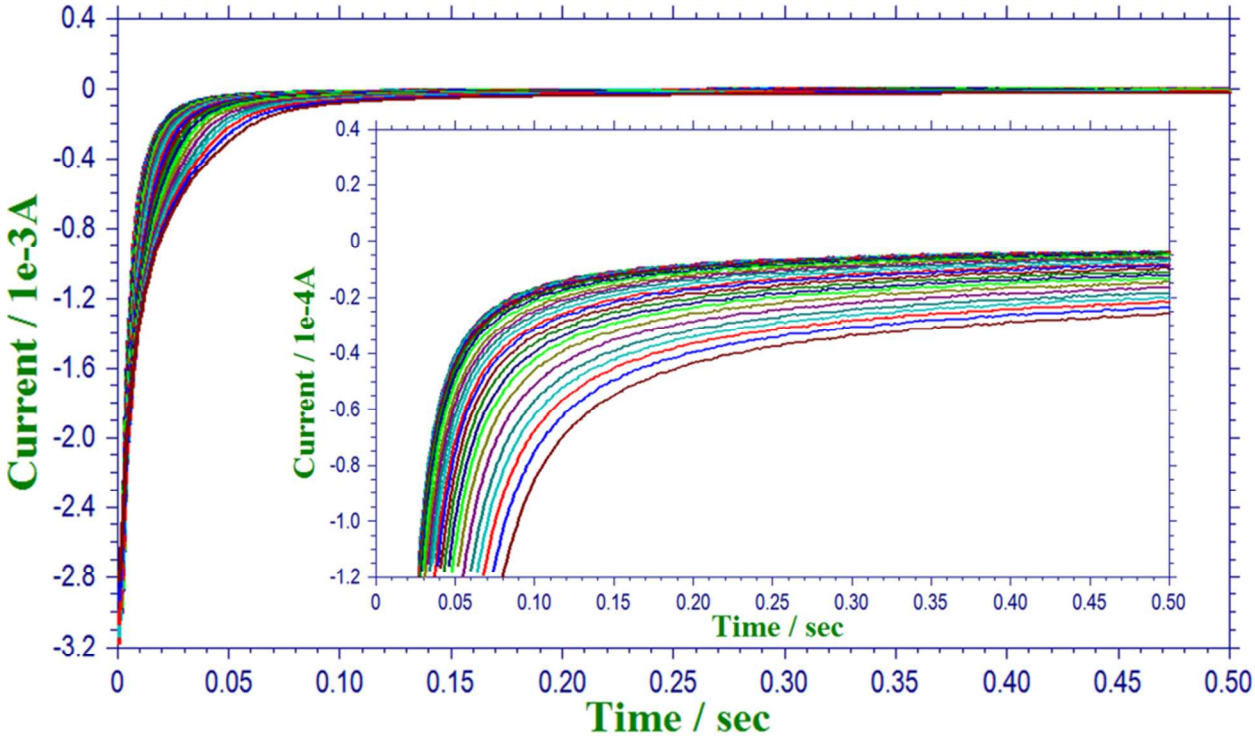

Fig. 6a

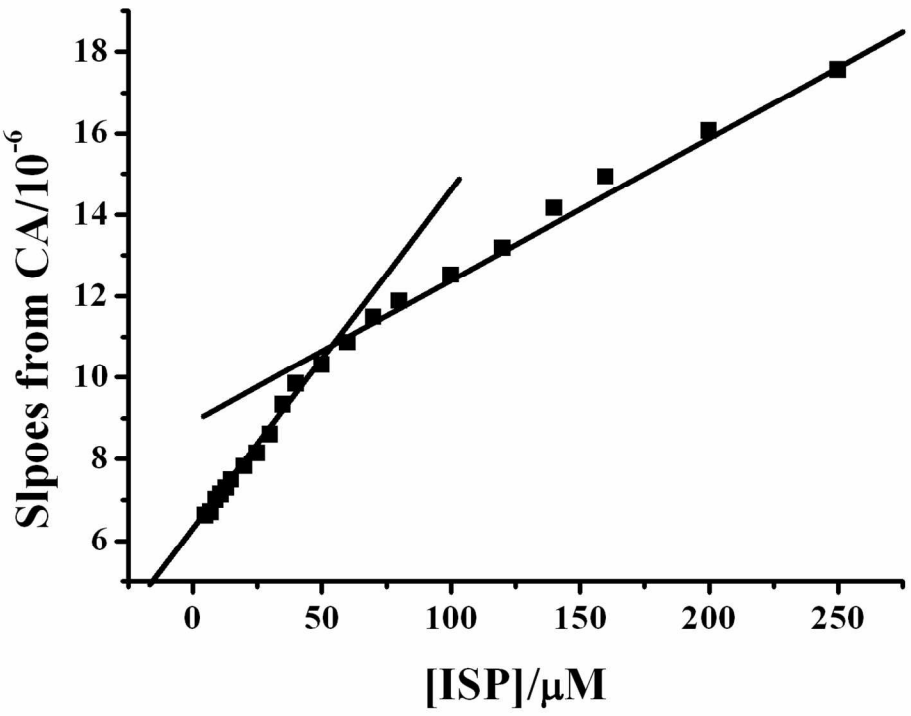

Fig. 6b

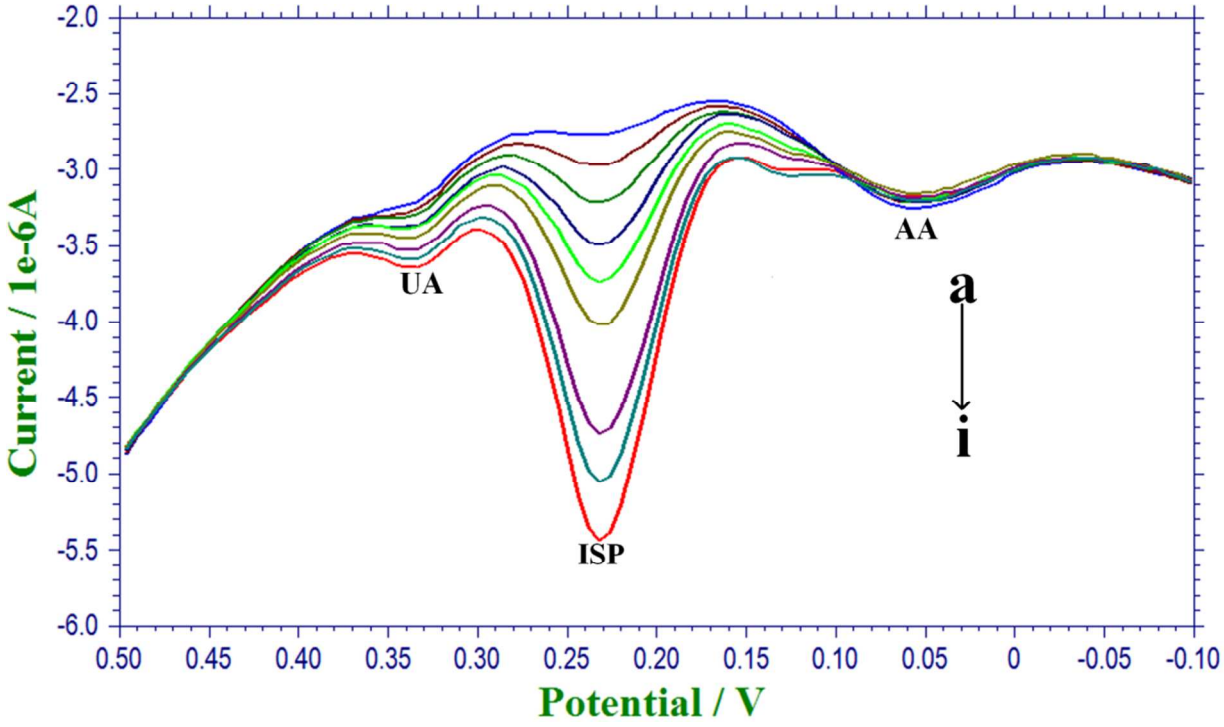

Fig. 7a

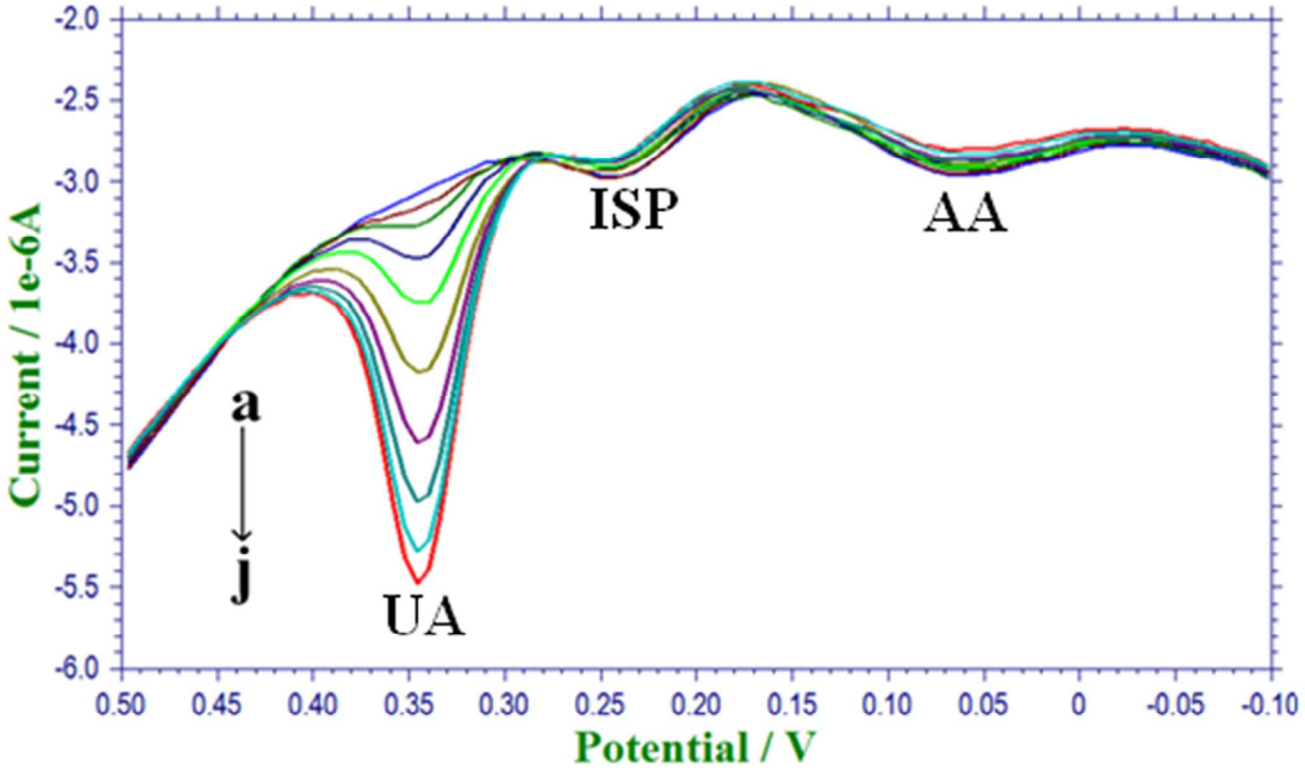

Fig. 7b

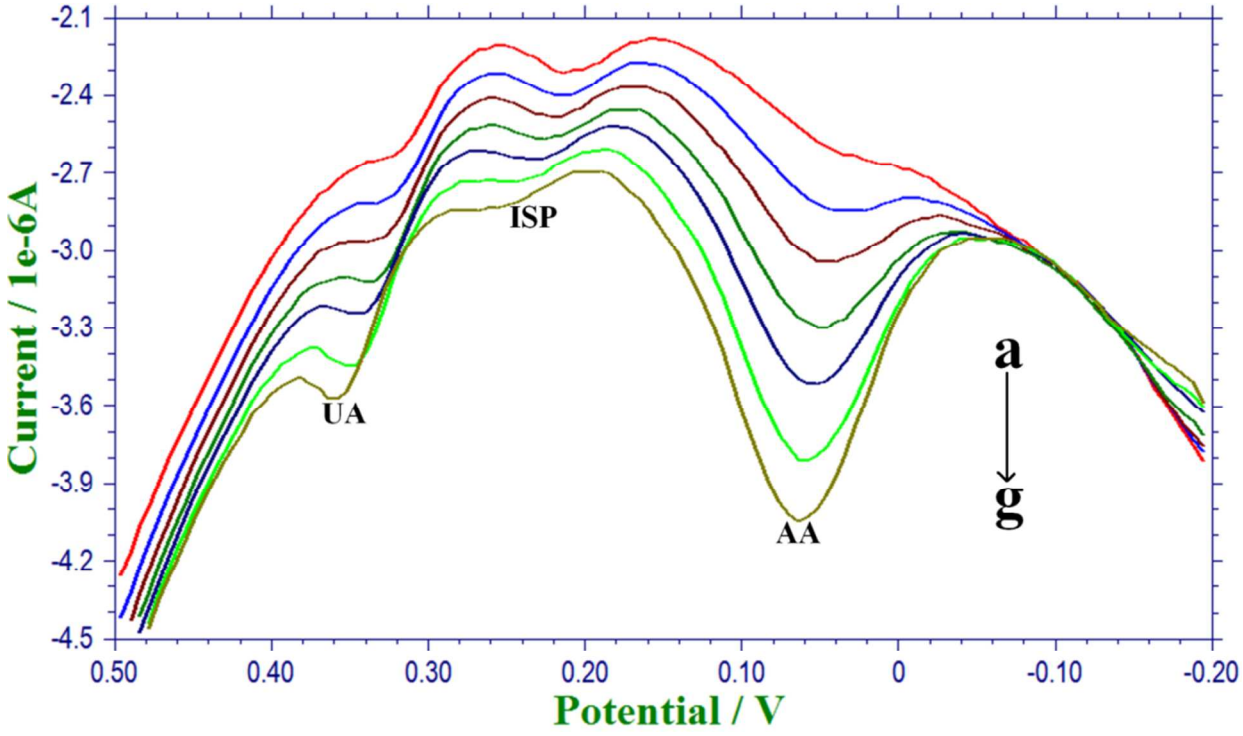

Fig. 7c

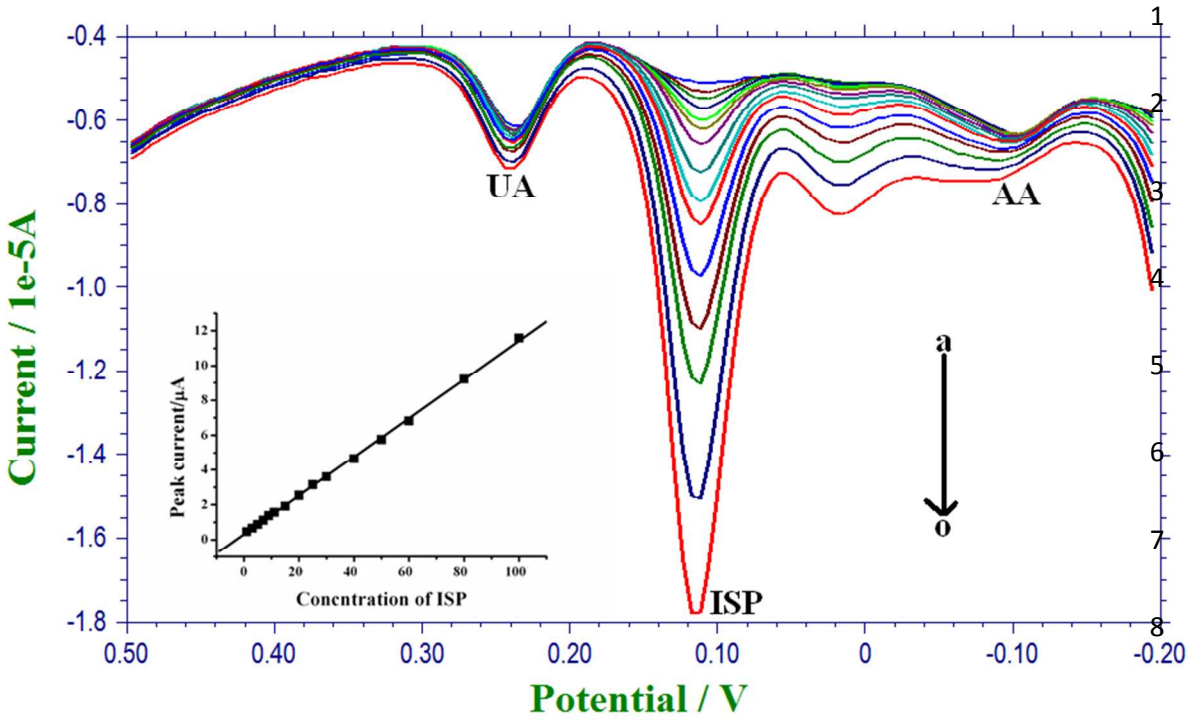

Fig. 7d

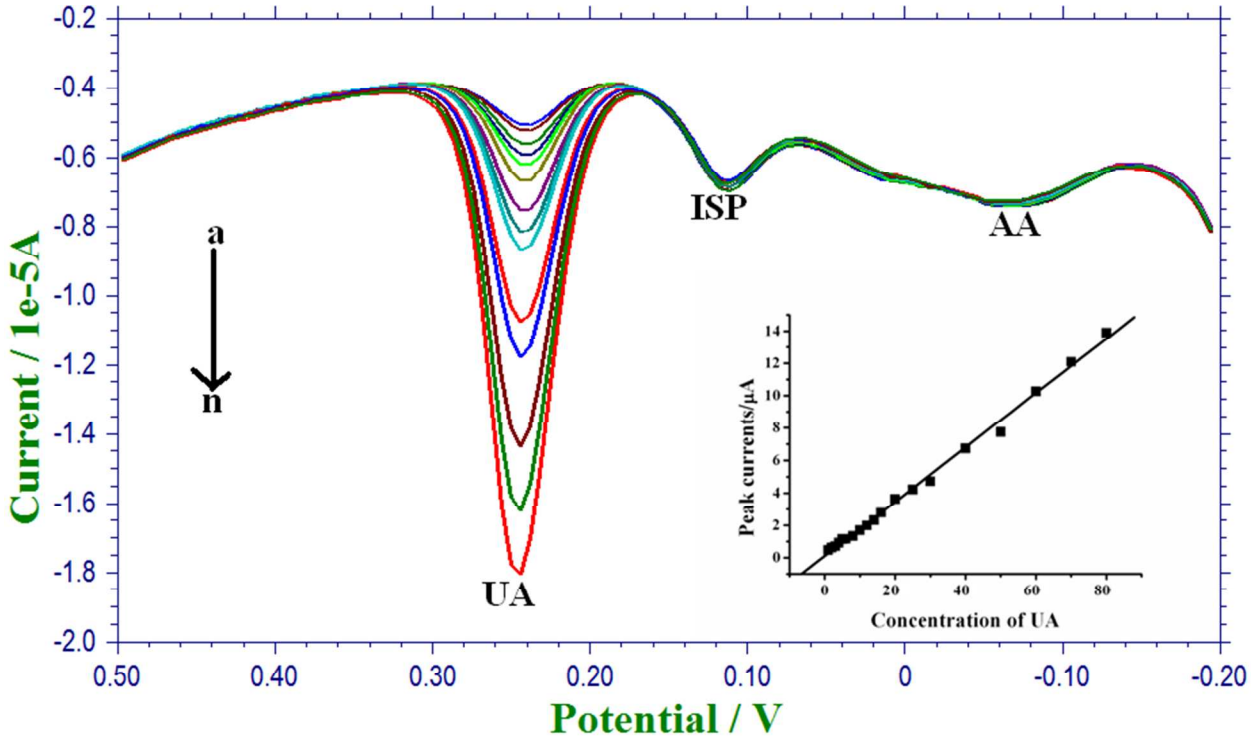

Fig. 7e

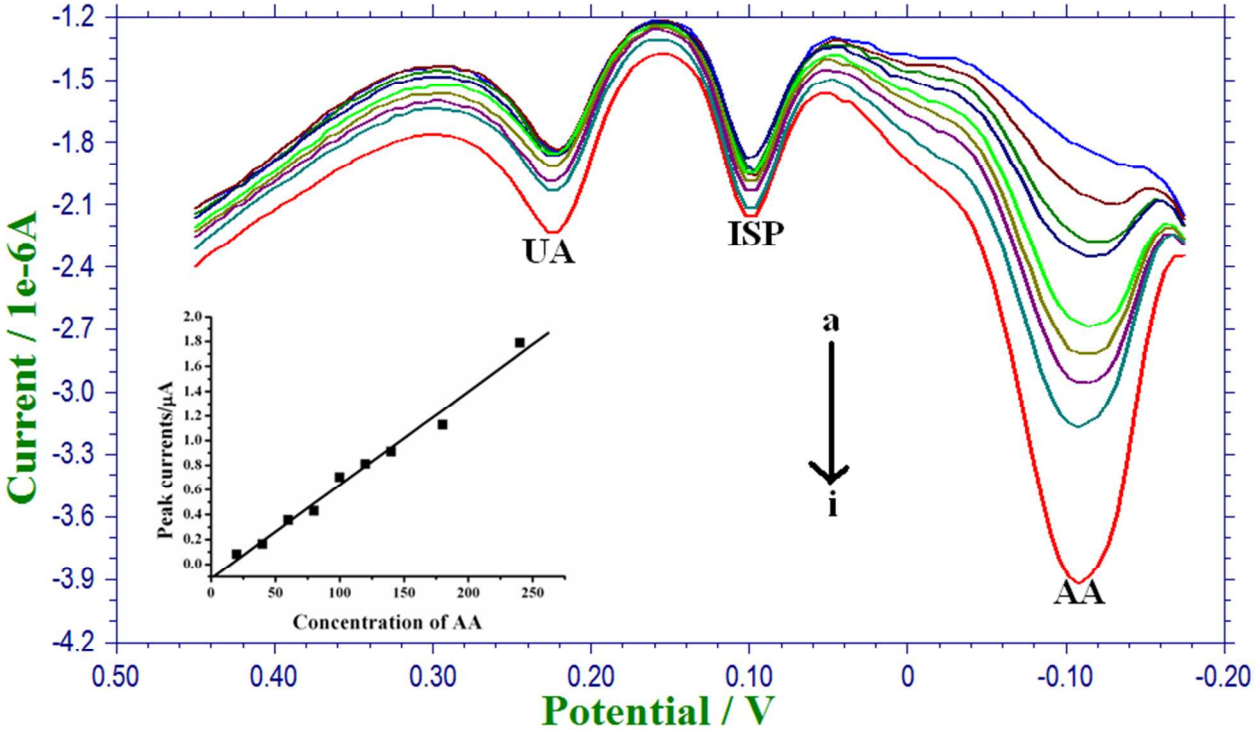

Fig. 7f

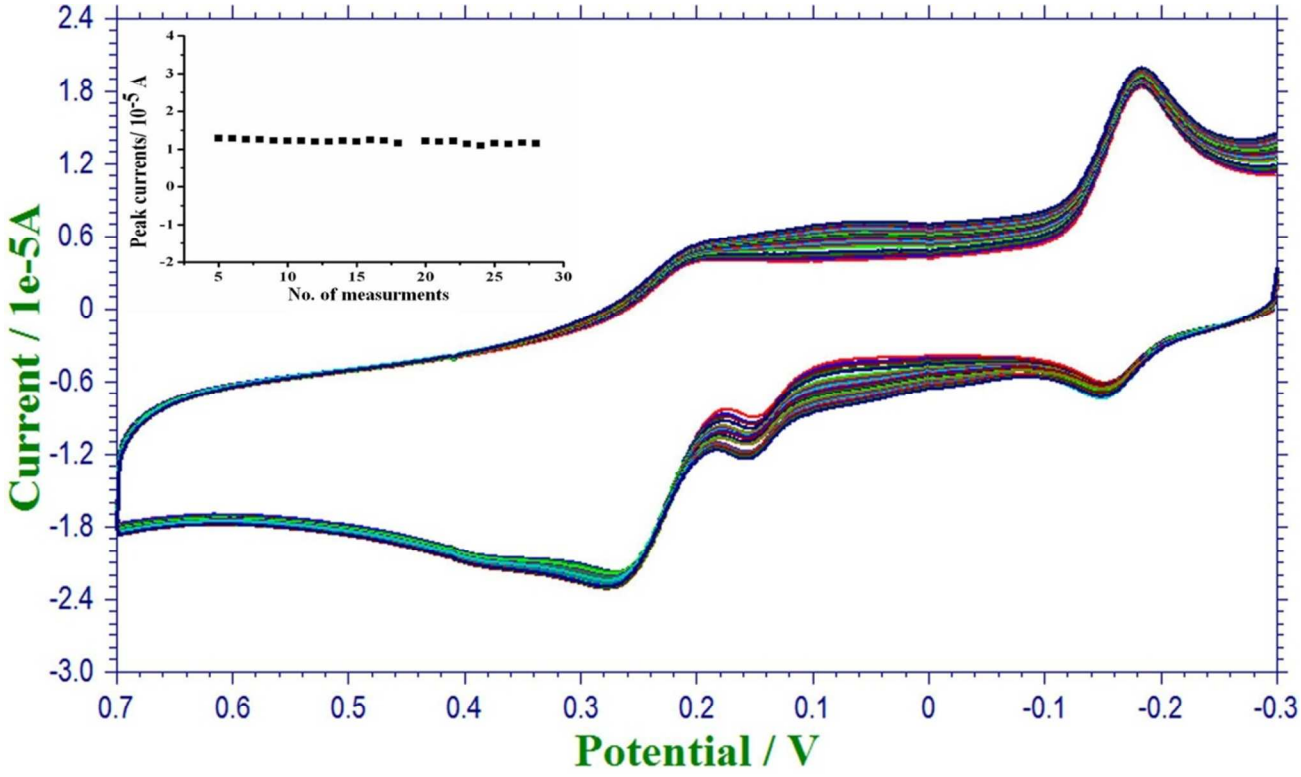

Fig. 8

Scheme 1: Schematic representation of enzyme activity

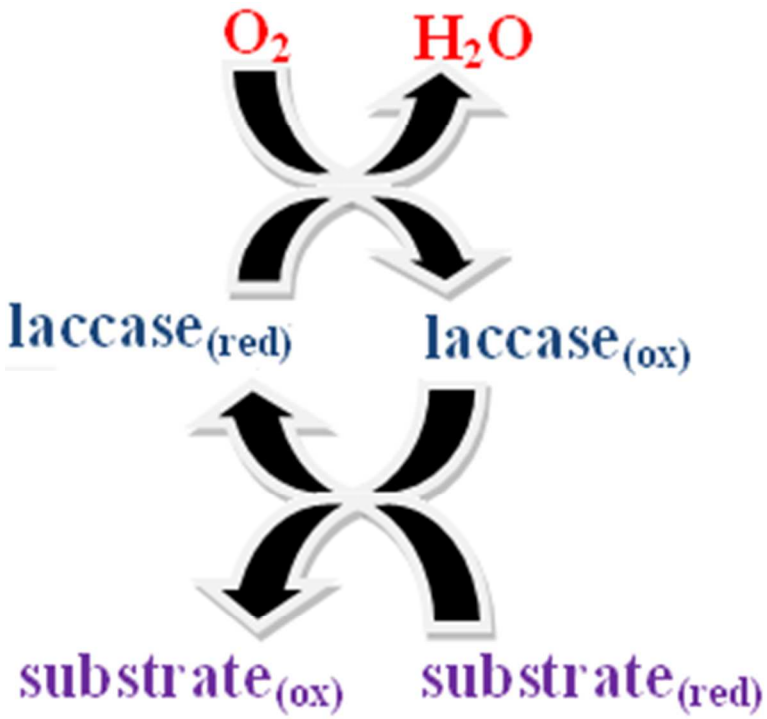

Scheme. 2: Electrochemical redox mechanism of Isoprenaline

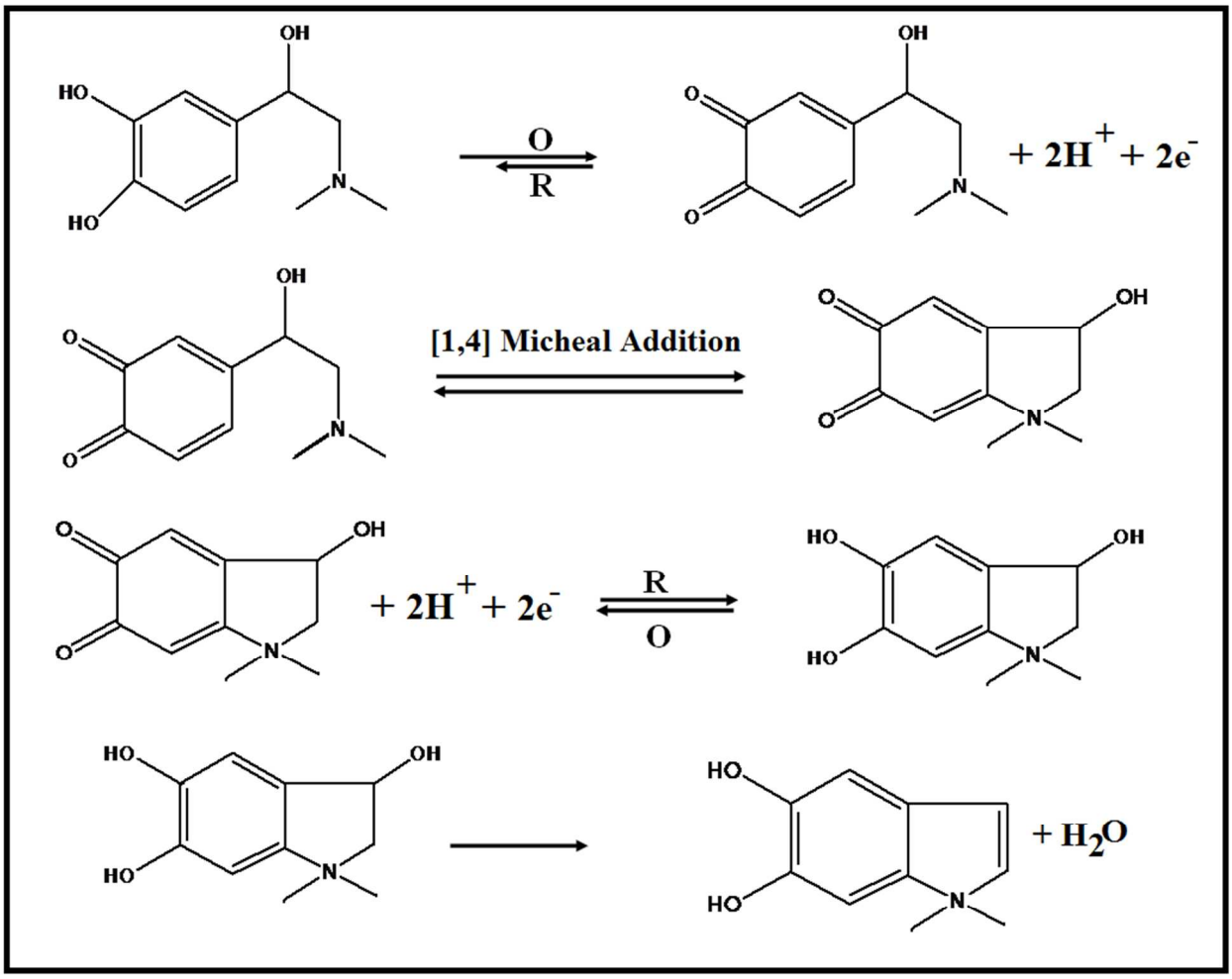

Tables:

Table. 1: Various parameters determined for $[Fe(CN)_6]^{-3}$ at three different electrodes

Electrode	Diffusion coefficient (cm^2s^{-1})		Surface area	I_p^a/i_p^c
	D_o	D_r	(mol/cm^2)	
Bare GEC	2.56×10^{-6}	2.46×10^{-6}	2.38×10^{-9}	0.98
MWCNT/GCE	2.78×10^{-6}	2.61×10^{-6}	2.56×10^{-9}	1.01
Lac-SiSG/MWCNT/GCE	3.79×10^{-6}	3.8×10^{-6}	3.32×10^{-9}	0.99

Table. 2: EIS data received from circuit fitting for three different electrodes.

Electrode	R_{sol}/Ω	C/μF	R_{ct}/Ω	W
Bare GCE	19.09	0.86	289.4	0.00015
MWCNT/GCE	21.04	10.68	0.001	0.00018
Lac-SiSG/MWCNT/GCE	21.49	16.43	0.001	0.00014

Table. 3 Comparison table for the determination of ISP with different methods.

Methods	Detectection	LDR (μML^{-1})	LOD (μML^{-1})	Ref
CV[a]	CuHCF[d]	196 – 1070	80	2
Spectrophotometry	Silica reactor	123 – 738	62.5	26
Chemiluminescence	-	0.94 – 236	0.236	31
HPLC[b]	Chemiluminescence	-	0.00016	48
DPV[c]	1-Butyl-3-methylimidazolium hexafluoro phosphate	1.0 – 520.0	0.85	49
DPV	LacSiSG/MWCNT/GCE	50.0 - 250.0	0.18	Present work

[a]Cyclic voltammetry

[b]High performance liquid chromatography

[c]Differential pulse voltammetry

[d]Copper(II) hexacyanoferrate(III)

Table. 4: Determination of ISP in ISP injection samples at serum and buffer solutions.

medium	Added (μM)	Found (μM)	Recovery (%)	Bias (%)
Buffer	40	41.7	104.25	+4.25
	60	61.1	101.83	+1.83
	80	80.6	100.75	+0.75
Serum sample	40	39.31	98.28	-1.72
	60	57.2	95.33	-4.67
	80	77.5	96.88	-3.12

Graphical abstract: